ELSEVIER

Journal of Chromatography A, 730 (1996) 247–259

JOURNAL OF CHROMATOGRAPHY A

Transient electrophoretic processes in capillaries of non-uniform cross-section

K. Šlais

Institute of Analytical Chemistry, Academy of Sciences of the Czech Republic, 611 42 Brno, Czech Republic

Abstract

The previous model of electrofocusing in a tapered capillary was extended to cover both focusing and non-focusing modes of capillary electrophoresis. The more general equation derived can be used either for tapered or for funnel-like segments of capillary for which the product of the local cross-section and the length-based separation coordinate is constant. The particular forms of the equation are used to discuss the changes in the variance of a moving Gaussian zone in practically interesting cases of electrophoresis in a capillary of non-uniform cross-section.

Keywords: Capillary electrophoresis; Capillary columns; Column geometry

1. Introduction

Transient electrophoretic effects are understood here as changes in volume and/or width of the Gaussian concentration profile. The simplest case is zone electrophoresis in a capillary of uniform cross-section. Further, more pronounced transitions occur when electrophoresis is carried out in capillaries of non-uniform cross-section. Such instances are interesting from several points of view. They may bring some interesting features, namely in the focusing modes of electrophoresis [1–6]. Also, non-uniform capillary geometry could extend the applicability of detection schemes [7–9]. However, non-uniform capillaries may bring excessive band broadening, as found in the case of a bubble detection cell [8] or in the coupling of capillary limbs of Y- or T-pieces [10]. In order to minimize the dispersion, a smooth, gradual change in geometry is needed [7,8]. Transient processes also occur in focusing in a capillary of uniform cross-section when a step change of voltage is applied [11–14] or when the zone is transferred from a wide channel into a narrow capillary [5,15]. In such instances, the speed of approach to the steady state is of interest.

Recently, a model was suggested [1–3] which enables an estimate to be obtained of the width of a focused Gaussian zone which migrates in a capillary with a shallow taper. In the suggested model, a simplified analytical solution of the continuity equation is possible for the constant volume-based migration velocity and for the particular geometry for which the product of the length-based separation coordinate and the local cross-section is constant.

In this work, the previous model [1–3] was extended to obtain a more general equation for calculation of the time dependence of dispersion

0021-9673/96/$15.00
SSDI 0021-9673(95)01111-0

of a Gaussian zone in both focusing and non-focusing modes of electrophoresis. It can be applied to both a capillary of uniform cross-section and to a geometry specified in the model used. With the help of the derived equation, some practically interesting transient processes are discussed.

2. Theory

The continuity equation is a partial differential equation that will, upon solution, yield the concentration as a function of time and distance. It was shown [16] that diffusion and diffusion-like processes transform initial zones into Gaussian zones in most practical cases. Thus, the Gaussian function is the desired mathematical solution to the differential equation. In the following treatment, the changes in the environment influencing the shape of the concentration profile are such that the changes in the zone shape can be described in terms of parameters of a Gaussian curve. In other words, the zone variance can be treated as a variable. For shallow, smooth changes in a capillary cross-section, the continuity equation was approximated [1] by a balance of dispersion and focusing fluxes within the Gaussian zone.

The equation for an actual length-based variance, σ^2, of the Gaussian zone which migrates in a constant gradient of migration velocity, dv/dy = constant, and with a constant diffusion coefficient, D = constant, can be written as [1]

$$\frac{D^* - D}{\sigma^2} = \frac{dv}{dy} \tag{1}$$

where the effective dispersion coefficient, D^*, is related to the changes in volume of the Gaussian zone by

$$D^* = \frac{\bar{v}}{2A} \cdot \frac{d\sigma_V^2}{dV} \tag{2}$$

where A is the local cross-section, $\bar{v}$ is the mean local velocity of the zone centre, $\bar{v} = dy/dt$, σ_V^2 is the volume-based variance of the Gaussian zone, dV is the element of displaced volume, $dV = \Phi\, dt$, and Φ is volume-based velocity of the zone, $\Phi = A\bar{v}$. Under a constant electric current, I, Φ is constant. Since, in a capillary with a shallow taper, $\sigma_V = A\sigma$, we may write for the effective dispersion coefficient

$$\frac{D^*}{\sigma^2} = \frac{\bar{v}}{2}\left(\frac{d \ln \sigma^2}{dy} + \frac{d \ln A^2}{dy}\right) \tag{3}$$

By insertion of Eq. 3 into Eq. 1, we obtain after rearrangement

$$\frac{d \ln \sigma^2}{dt} = \frac{2dv}{dy} - \frac{2d \ln A}{dt} + \frac{2D}{\sigma^2} \tag{4}$$

The solution of Eq. 4 may be simplified for the special shape of the capillary for which Ay = constant. Let us consider a segment of the tapered capillary of length $L = y_d - y_0$ and volume V_L, over which the cross-section changes from A_0 to A_d (see Fig. 1). Then, the shape of the capillary segment can be specified by the equation

$$Ay = \frac{V_L}{\ln q} \tag{5}$$

where

$$V_L = \int_{y_0}^{y_d} A\, dy \tag{6}$$

and q is the ratio of the inlet cross-section, A_0, to the outlet cross-section, A_d:

$$q = \frac{A_0}{A_d} \tag{7}$$

When a capillary of circular cross-section is considered, the ratio of the inlet radius, r_0, to the outlet radius, r_d, is $r_0/r_d = \sqrt{q}$. It follows from Eqs. 5–7 that A is related to the displaced volume, V, by

$$\ln\left(\frac{A_0}{A}\right) = \frac{V \ln q}{V_L} \tag{8}$$

For a shape of the capillary defined by Eqs. 5–7 and for a constant Φ, the second term of the RHS of Eq. 4 is a constant and we may write

$$-\frac{d \ln A}{dt} = \frac{\ln q}{t_L} \tag{9}$$

where t_L is the time needed for migration of the zone from $y = y_0$ to $y = y_d$, $t_L = V_L/\Phi$. After insertion of Eq. 9 into Eq. 4 and rearrangement, we obtain

$$\frac{d\sigma^2}{dt} = 2\sigma^2\left(\frac{dv}{dy} + \frac{\ln q}{t_L}\right) + 2D \tag{10}$$

According to the model adopted, the last equation contains only two variables, namely σ^2 and t. After their separation, the equation can be integrated and we obtain

$$\ln\left(\frac{\sigma^2 - Z}{\sigma_0^2 - Z}\right) = \frac{-2Dt}{Z} \tag{11}$$

where t is the time of zone migration through the considered segment of tapered capillary, $0 < t < t_L$, σ_0^2 is the length-based peak variance at the beginning of the considered segment where $y = y_0$, $A = A_0$, $t = 0$ (see Fig. 1), and Z is a constant given by

$$Z = \frac{-D}{\frac{dv}{dy} + \frac{\ln q}{t_L}} \tag{12}$$

Eq. 11 can be rearranged to the form which will also be used for the discussion of the particular cases:

$$\sigma^2 = \sigma_0^2 e^{\frac{-2Dt}{Z}} - Z\left(e^{\frac{-2Dt}{Z}} - 1\right) \tag{13}$$

Although the applicability of this equation is limited by the particular shape of the capillary, it may be used at least for a semi-quantitative estimation of the dispersion of the Gaussian zone in practically interesting transient processes.

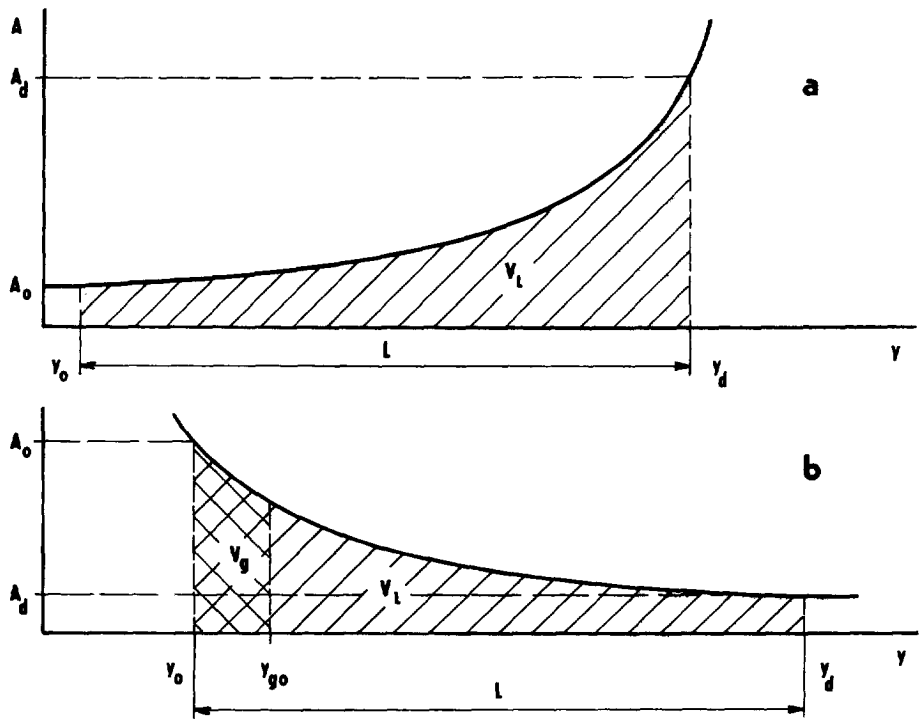

Fig. 1. Definition of the capillary shape. (a) Funnel-shaped capillary; (b) tapered capillary. y = Longitudinal separation coordinate; A = variable cross-section; A_0 and A_d = capillary cross-section at the inlet point, y_0, and at the detection point, y_d, respectively; L = capillary length; V_L = capillary volume; V_g = volume of moving natural pH gradient; $y_{g0}-y_0$ = part of the capillary occupied by sampled solution at the beginning of the electrophoretic run.

3. Discussion

3.1. The case of $Z = \pm\infty$

In a capillary of constant cross-section, q approaches unity and ln q is zero. Further, when no mobility gradient is used, then $dv/dy = 0$. According to Eq. 12, Z approaches infinity and the exponents in Eq. 13 tend to zero. Then, e^x may be expanded as $1 + x$ and Eq. 13 changes to the description of zone dispersion in zone electrophoresis in a capillary of uniform cross-section (CZE):

$$\sigma^2 = \sigma_0^2 + 2Dt \tag{14}$$

as expected. The same result is obtained also for dispersion of the zone in a capillary without applied voltage, when $dv/dy = 0$ and t_L approaches infinity. The example may be found in defocusing of a zone in isoelectric focusing (IEF) after switching the voltage off [11–13].

3.2. The case of $Z = -(Dt_L)/(\ln q)$

Let us discuss the migration of a Gaussian zone in a capillary of non-uniform cross-section, when no gradient of pH and/or mobility is used. Then, $q \neq 1$ and $dv/dy = 0$. Such a model can be applied for CZE in a capillary of non-uniform cross-section with the geometry specified by Eqs. 5–7. It follows from Eq. 12 that

$$Z = \frac{-Dt_L}{\ln q} \tag{15}$$

Insertion of Eq. 15 into Eq. 13 gives the length-based variance of the peak as a function of migration time, t $(0 < t < t_L)$:

$$\frac{\sigma^2}{\sigma_0^2} = q^{2t/t_L} + \frac{2Dt_L}{\sigma_0^2}\left(\frac{q^{2t/t_L} - 1}{2 \ln q}\right) \tag{16}$$

For $q > 1$, which means a continuous decrease of A with increasing y, the length-based zone variance increases rapidly; the larger is q, the faster is the increase in zone length.

The case with $q < 1$ is more interesting. It means a continuous increase in the local cross-section with the separation coordinate. Such an instance may model the funnel-shaped capillary or part of the limb in a Y-piece or the front part of a bubble detection cell on a capillary (see Fig. 2).

Eq. 16 describes the variation of the length-based zone variance with time; with constant I, it can describe the peak variance as a function of the displaced volume, V. The dependence of the relative change of peak variance on the displaced volume is illustrated in Fig. 3a for two values of q ($q = 0.1$, $r_d/r_0 = 3.2$, and $q = 0.04$, $r_d/r_0 = 5$) and for the parameter $(2Dt_L)/\sigma_0^2$ set to 0.01. Indeed, owing to the first term on the RHS of Eq. 16, the length-based variance decreases with migration of a zone into positions with a larger cross-

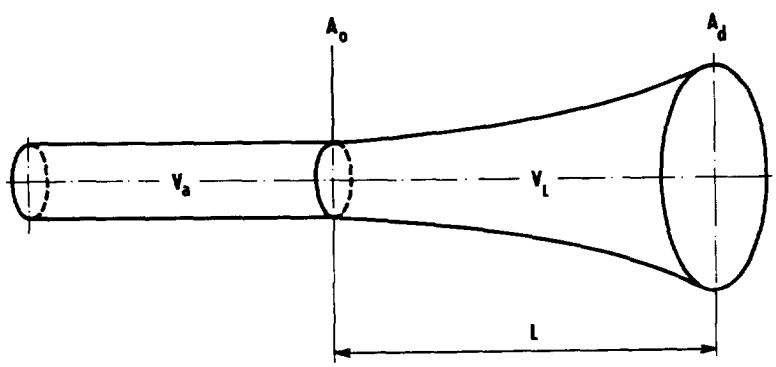

Fig. 2. Coupling of a uniform capillary to a funnel-shaped capillary. V_a = Volume of the uniform separation capillary; other symbols as in Fig. 1.

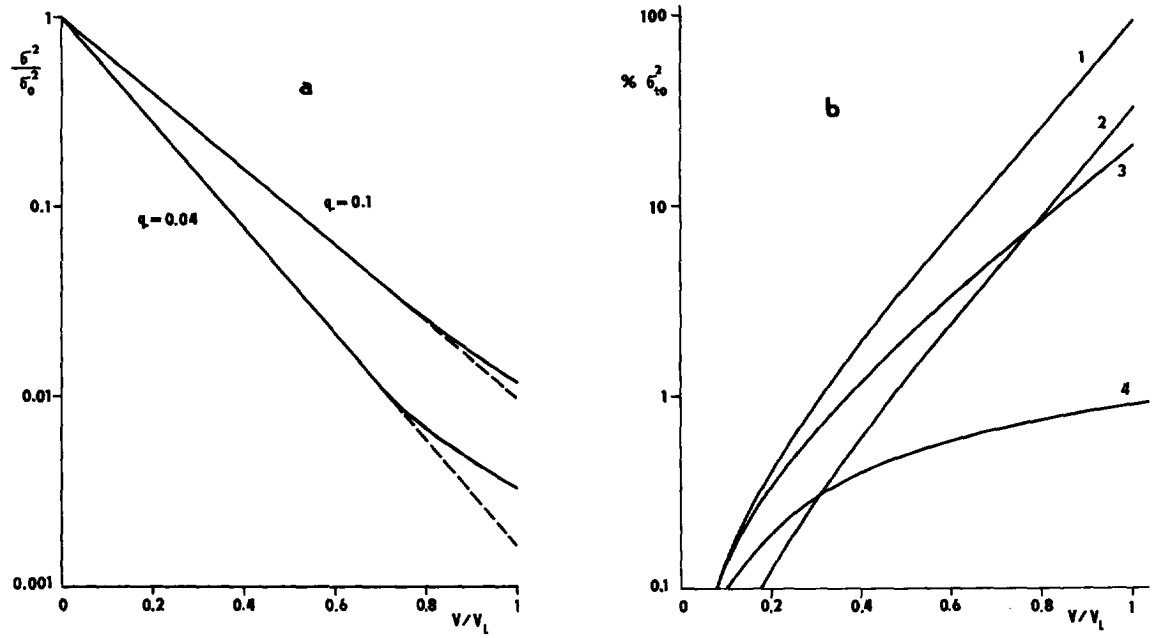

Fig. 3. Dependence of the peak variance in CZE in a funnel-shaped capillary on the displaced volume. (a) Length-based variance calculated from Eq. 16 for $2Dt_L/\sigma_0^2 = 0.01$; (b) contribution of funnel-shaped capillary to the time-based peak variance calculated from Eq. 19 as a percentage of the inlet-time based peak variance, σ_{t0}^2. Curves: (1) $q = 0.04$, $t_L/t_a = 0.01$; (2) $q = 0.04$, $t_L/t_a = 0.003$; (3) $q = 0.1$, $t_L/t_a = 0.01$; (4) $q = 1$, $t_L/t_a = 0.01$. V = Displaced volume; σ^2/σ_0^2 = ratio of actual length-based peak variance to the inlet peak variance at $y = y_0$; q = ratio of the inlet to the detection cross-sections ($q = A_0/A_d$); other symbols as in Fig. 1.

section. This effect was recently suggested for sensitivity enhancement of optical detection [7–9]. Actually, the first term on the RHS of Eq. 16 expresses the conservation of the zone volume, while the second represents the contribution of the capillary segment concerned with diffusion spreading. When, owing to a small t_L or a large σ_0^2, the second term in the RHS of Eq. 16 is very small in comparison with the first, the equation expresses only the reduction of the length-based variance in accordance with the increase in the cross-section, as discussed previously [7,8] (see also the straight lines in Fig. 3a). This dependence can also be derived directly from Eq. 3 for $D^* = 0$.

However, it can be seen from Fig. 3a that there is a positive departure of the actual peak variance from this simple relationship when the zone approaches places with a large cross-section. The departure is caused by the second term on the RHS of Eq. 16; it becomes more apparent when we discuss the time-based zone variance which is actually observed on the separation record. The time-based zone variance σ_t^2 is given by

$$\sigma_t^2 = \frac{\sigma^2}{\bar{v}^2} \tag{17}$$

With the use of Eqs. 8 and 17, we obtain for constant $\Phi = A\bar{v}$

$$\sigma_t^2 = \frac{\sigma^2}{\bar{v}_0^2} q^{-2t/t_L} \tag{18}$$

where $\bar{v}_0$ is the mean linear velocity of the zone at the inlet of the considered segment of the funnel-shaped capillary, where $y = y_0$ and $A = A_0$ (see Fig. 2). In order to show the contribution of the funnel-like segment to the overall time-based variance, it is useful to relate σ_t^2 to the inlet time-based variance, σ_{t0}^2. As long as σ_0^2 is generated by zone electrophoresis in a capillary of constant cross-section, we may relate σ_0^2 to the

time of zone electrophoresis, t_a, as $\sigma_0^2 = 2Dt_a$. Thus, the inlet time based variance, σ_{t0}^2, is $\sigma_{t0}^2 = 2Dt_a/\bar{v}_0^2$. With the use of this relationship, and by insertion of Eq. 16 into Eq. 18, we obtain for time based zone variance, σ_t^2,

$$\frac{\sigma_t^2}{2Dt_a/\bar{v}_0^2} - 1 = \frac{t_L}{t_a}\left(\frac{1 - q^{-2t/t_L}}{2 \ln q}\right) \tag{19}$$

The RHS of Eq. 19 estimates the magnitude of the relative contribution of the funnel-shaped capillary to the overall time-based variance of the zone. The term in parentheses is a shape factor which indicates the increase in band broadening due to the migration in the particular shape relative to the capillary of uniform cross-section with volume V_L and cross-section A_0. Since $t/t_L = V/V_L$ and $t/t_a = V/V_a$, the relative change in the local σ_t^2 with the displaced volume can be illustrated by Fig. 3b.

In order to show the effect of the magnitude of an increase in the capillary cross-section, let us compared curves 1,3 and 4 in Fig. 3b in which r_d/r_0 equals 5, 3.2 and 1, respectively, and the ratio of the volume of the funnel-shaped segment to the volume of the separation capillary, V_L/V_a has been set to 0.01 in all three cases. It is apparent that a funnel-shaped segment can contribute considerably to the overall time-based variance of the zone. For example, with $q = 0.1$, which means $r_d/r_0 = 3.2$ (curve 2), the term in parentheses on the RHS of Eq. 19 amounts to 21.5 at $y = y_d$. With $q = 0.04$ and $r_d/r_0 = 5$ (curve 1), it increases to 100. Thus, if the volume of the front part of bubble cell, which may be about one third of the entire bubble cell volume, amounts to 1% of the volume of the separation capillary, the time-based variance generated in the detection cell is comparable to the variance generated in the separation capillary. In comparison with a uniform capillary segment of the same V_L (see curve 4), the increase in the time-based variance is about 100 times larger. The possible way out may be to reduce the volume of the funnel-shaped segment (see curves 1 and 2), where the increase in the cross-section is the same, $q = 0.04$, but the volume of the segment is 3.3 times smaller for curve 2 in comparison with curve 1. However, the use of too small a cell volume acts against the demand for smooth changes in geometry. In the limiting case of step changes in the cross-section, the bubble cell could be approximated by a reaction chamber. Therefore, it is not surprising that a bubble cell with a 15-fold increase in diameter was found to be unsuitable for detection [8].

Although the above equations were derived with strong simplifications, the results obtained indicate the possible limits in the use of funnel-shaped capillaries in electrophoresis. Qualitatively, the strong increase in zone dispersion can be explained as follows: the increase in the cross-section leads to a decrease in the length-based width of the zone (see the first term on the RHS of Eq. 16). However, the decrease leads to an increase in the axial concentration gradients which speed up the longitudal diffusion fluxes (see the second term on the RHS of Eq. 16). Their effects are also proportional both to the increase in the cross-section (see the parameter q) and to the total time spent in the funnel-shaped capillary (see the parameter t_L or V_L).

Since the separate contributions to the overall zone dispersion are additive [16], the dispersion in the shapes which are different from those specified by Eqs. 5–7 can be approximated by the sum of the individual dispersions in the segments connected in series. For instance, the dispersion at the outlet of the bubble cell may be approximated by the dispersion in a conduit composed of a funnel-shaped segment, a segment with a constant cross-section and a tapered segment. Also, such an approximation can be used to estimate of the dispersion in a Y- or T-piece.

3.3. The case of $Z = -D/(dv/dy)$

Let us discuss the changes in the peak variance during focusing in a capillary with a uniform cross-section. Then, $dA/dy = 0$, $q = 1$ and $dv/dy \neq 0$. Accordingly, Eqs. 11 and 13 model the relaxation of a focused peak. Of practical interest may be the cases in which, e.g., the voltage is changed stepwise or the zone is transferred from a tapered capillary with the geometry specified

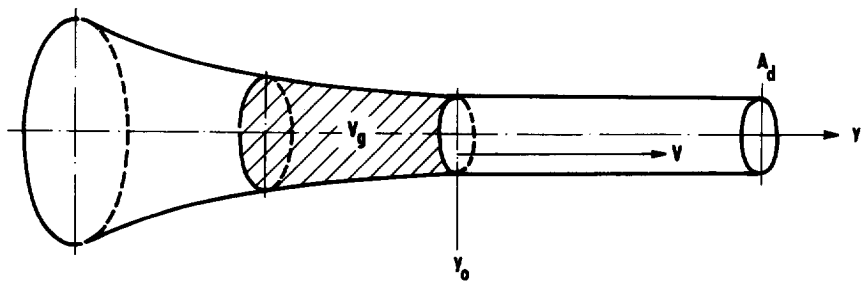

Fig. 4. Coupling of a tapered capillary to a capillary of uniform cross-section. Symbols as in Fig. 1.

by Eqs. 5–7 to a capillary of uniform cross-section (see Fig. 4).

In electrophoresis in a capillary of uniform cross-section, the velocity gradient is a product of the field strength and the mobility gradient, $dv/dy = E\, d\mu/dy$. From Eq. 12, the Z term then has the form

$$Z = \frac{-D}{E\dfrac{d\mu}{dy}} \tag{20}$$

Usually in electrofocusing, $dv/dy < 0$, so that $Z > 0$. From the simplified model of IEF [17–18], it follows for the length-based variance of a Gaussian zone under steady-state conditions that

$$\sigma_s^2 = \frac{-D}{E\dfrac{d\mu}{dy}} \tag{21}$$

Since the denominator on the RHS of Eq. 21 is constant, the steady state can be reached also for a migrating focused zone [19]. From comparison of Eqs. 20 and 21, it is apparent that $Z = \sigma_s^2$ for $Z > 0$. By insertion of Eqs. 20 and 21 into Eq. 13 we obtain for the relaxation of a Gaussian zone during focusing in a capillary of constant cross-section

$$\sigma^2 = \sigma_0^2\, e^{-2Dt/\sigma_s^2} - \sigma_s^2\left(e^{-2Dt/\sigma_s^2} - 1\right) \tag{22}$$

Clearly, if $\sigma_0^2 = \sigma_s^2$, Eq. 22 reduces to $\sigma^2 = \sigma_s^2$, which means the steady state determined by Eq. 21. Also, if σ_s^2 becomes very large (or infinite, e.g., when the voltage is switched off), for $\sigma_0^2 \ll \sigma_s^2$, Eq. 22 becomes the equation of pure diffusion spreading (see Eq. 14).

Eq. 22 is identical with the equation for relaxation of zones in IEF derived previously [11,12] with the use of more involved mathematics [20]. It was early recognized from the experiments [14] and verified by computer modelling [21–23] that this equation is not generally applicable to the early stages of IEF. It was found that the initially flat concentration profile transforms into two transient peaks which arise at the ends of the initially rectangular concentration pulse, migrate toward each other and finally merge. It was also found [21] that Eq. 22 can describe the dynamics of the focusing process if the final position of the focused zone is in the centre of the segment in which natural gradient is generated, and if σ_s is not much smaller then the initial length of the flat concentration profile, L_{g0}, which is $L_{g0} = V_g/A$ where V_g is the volume of the generated natural pH gradient. For $L_{g0}^2/\sigma_s^2 = 50$, it was found [21] that the flat profile transforms directly into a single peak and an error of less than 1% will result from assuming linearity of the performed mobility gradient. Similarly, $L_{g0}^2/\sigma_s^2 = 200$ makes an error of 10% or less. With the use of relationship for the variance of the rectangular profile, $\sigma_{Lg}^2 = L_{g0}^2/12$, it appears that Eq. 22 can be used for the approximation of focusing dynamics of a Gaussian zone for which $0 < \sigma^2/\sigma_s^2 < 15$. When the pH of zone centroid remains constant, Eq. 22 can also be used for focusing of moving zones.

For the evaluation of some practically interesting cases of focusing during the migration in

capillary, let us introduce for the local mobility gradient [1]

$$\frac{d\mu}{dy} = \frac{d\mu}{d(pH)} \frac{\delta(pH)}{V_g} \cdot A \quad (23)$$

where $d\mu/d(pH)$ is the steepness of the mobility vs. pH dependence of the considered compound [$d\mu/d(pH) < 0$ for electrofocusing] and $\delta(pH)/V_g$ is the volume-based steepness of the linear natural pH gradient, which is the pH difference, $\delta(pH)$, over the respective segment of gradient volume V_g. Further, since $\Phi = A\bar{v}$ and $\bar{v}$ can be written as $\bar{v} = \bar{\mu}E$ for a capillary of constant cross-section, we may write Eq. 22 or Eq. 11 in the form

$$\frac{\sigma^2}{\sigma_s^2} - 1 = \left(\frac{\sigma_0^2}{\sigma_s^2} - 1\right) \times \exp\left[2\delta(pH) \cdot \frac{d\mu/d(pH)}{\bar{\mu}} \cdot \frac{V}{V_g}\right] \quad (24)$$

The calculated change in the ratio of the actual peak variance to the steady-state peak variance, σ^2/σ_s^2, is shown in Fig. 5 as a function of the displaced volume, V, which is expressed as a multiple of V_g. The parameters in Eq. 24 were chosen as $\sigma_0^2/\sigma_s^2 = 10$ and the term $\delta(pH)\{[d\mu/d(pH)]/\bar{\mu}\}$ equals -25 and -5 for curves 1 and 2, respectively. A rapid convergence of the peak width toward the steady state can be expected and a difference from the steady state within a few per cent can be achieved during the displacement of a fraction of V_g. It should be noted that the variance of peaks focused during their migration in a tapered capillary is expected to be larger than the local σ_s^2 only by few per cent [1–3], so that the condition $(\sigma_0^2/\sigma_s^2 - 1) \ll 1$ applies when the outlet of the tapered capillary is coupled to the cylindrical capillary (see Fig. 4). Hence only a very short cylindrical capillary should be sufficient for achieving an acceptably small departure from the steady state. This is advantageous for the design of a separation compartment in electrofocusing devices [5].

3.4. The case of Z expressed by Eq. 12

The gradient of migration velocity in a natural pH gradient moving in a tapered capillary specified by Eqs. 5–7 can be expressed as [1]

$$\frac{dv}{dy} = E \cdot \frac{d\mu}{dy} - \bar{\mu}E \cdot \frac{d \ln A}{dy} \quad (25)$$

The first term on the RHS of Eq. 25 is independent of the local cross-section. The increase in electric field strength caused by the

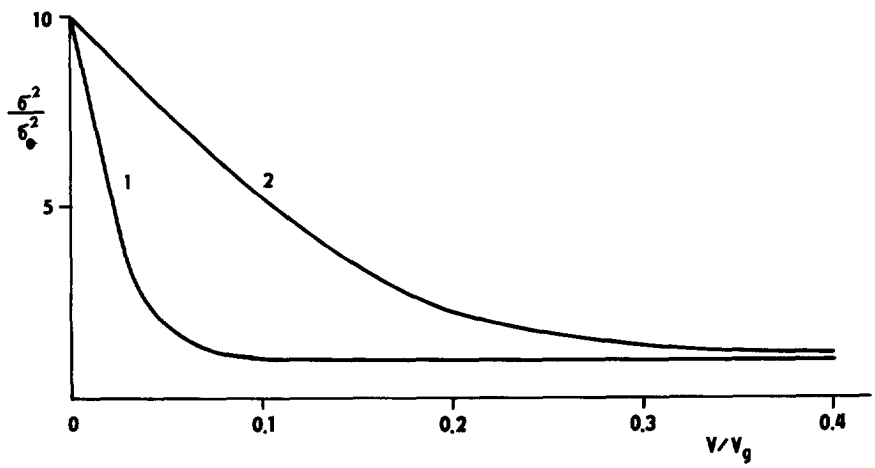

Fig. 5. Relaxation of a focused peak in a capillary of uniform cross-section calculated from Eq. 24 for $\sigma_0^2/\sigma_s^2 = 10$ and $\delta(pH)\{[d\mu/d(pH)]/\bar{\mu}\} = -25$ and -5 for curves 1 and 2, respectively. Symbols as in Figs. 1 and 3.

increase in current density at a position with a smaller cross-section is just counterbalanced by the same decrease in the length-based steepness of the pH gradient. The second term on the RHS of Eq. 25 is constant because of the capillary geometry has been specified by Eqs. 5–7. Thus, the dv/dy term is constant as introduced in Eq. 1. Further, for narrow bands and a shallow taper, it can be set $\bar{v} = \bar{\mu}E$ [1]. With use of Eqs. 9, 12 and 25 and $\bar{v} = dy/dt$, we obtain for the constant Z

$$Z = \frac{-D}{E \cdot \dfrac{d\mu}{dy} + \dfrac{2 \ln q}{t_L}} \tag{26}$$

Based on Eqs. 11, 13 and 26, a fast increase in the length-based variance can be expected for $Z < 0$; the higher is $q > 1$, the faster is the increase in the length-based variance with migration of the zone along the y coordinate. More interesting are the instances where $Z > 0$. In order to simplify the notation, let us introduce the constant variance of a zone focused in a tapered capillary, σ_ϵ^2, which is described by [1]

$$\sigma_\epsilon^2 = \frac{D}{E\left(\bar{\mu} \cdot \dfrac{2d \ln A}{dy} - \dfrac{d\mu}{dy}\right)} \tag{27}$$

The parameter σ_ϵ^2 is related to σ_s^2 through a constant coefficient, ϵ, by [1]

$$\epsilon = \left(1 - \frac{\sigma_s^2}{\sigma_\epsilon^2}\right) \tag{28}$$

With the use of Eqs. 9, 26 and 27 and $\bar{v} = \bar{\mu}E$, it appears that $Z = \sigma_\epsilon^2$ for $Z > 0$. Then, Eq. 13 can be rewritten as

$$\sigma^2 = \sigma_0^2 e^{-2Dt/\sigma_\epsilon^2} - \sigma_\epsilon^2\left(e^{-2Dt/\sigma_\epsilon^2} - 1\right) \tag{29}$$

When $\sigma_0^2 = \sigma_\epsilon^2$, σ^2 is constant, $\sigma^2 = \sigma_\epsilon^2$, as derived previously [1]. Further, when $\epsilon = 0$, which means $\sigma_\epsilon^2 = \sigma_s^2$ according to Eq. 28, Eq. 29 transforms to Eq. 22, which was discussed in Section 3.3.

With the use of Eqs. 23, 27 and 28, Eq. 29 or Eq. 11 can be written in the form

$$\frac{\sigma^2}{\sigma_\epsilon^2} - 1 = \left(\frac{\sigma_0^2}{\sigma_\epsilon^2} - 1\right) \times \exp\left[2(1-\epsilon)\delta(\mathrm{pH}) \cdot \frac{d\mu/d(\mathrm{pH})}{\bar{\mu}} \cdot \frac{V}{V_g}\right] \tag{30}$$

The parameter ϵ is related to the steepness of the capillary taper, the steepness of the pH gradient and the analyte mobility by [1]

$$\ln q = \frac{\epsilon}{2} \cdot \frac{-d\mu/d(\mathrm{pH})}{\bar{\mu}} \cdot \frac{\delta(\mathrm{pH})}{V_g} \cdot V_L \tag{31}$$

For $q \neq 1$ and $\epsilon \neq 0$, Eq. 31 can be substituted in Eq. 30 and we obtain

$$\frac{\sigma^2}{\sigma_\epsilon^2} - 1 = \left(\frac{\sigma_0^2}{\sigma_\epsilon^2} - 1\right) q^{\frac{2(\epsilon-1)}{\epsilon} \cdot \frac{t}{t_L}} \tag{32}$$

The instances with $\sigma_0^2 \neq \sigma_\epsilon^2$ described the relaxation of a focused Gaussian zone during its migration in a capillary with the geometry specified by Eqs. 5–7. Let us discuss two cases of practical interest.

The case of $q < 1$ and $Z > 0$

This condition expresses a the continuous increase in A with the separation coordinate which leads to $\epsilon < 0$ (see Eq. 31). Similarly to Section 3.2, the condition $q < 1$ leads to a discussion of the zone dispersion in a funnel-shaped segment of a capillary. However, instead of zone electrophoresis, focusing with mobilization is the mode of separation here.

Let us discuss the zone dispersion in the inlet part of a bubble detection cell (see Fig. 2). When we take the cross-section ratio $q = 0.1$ (i.e., $r_d/r_0 = 3.2$), then $\ln q = -2.3$. The volume of the funnel-shaped part, V_L, is substantially smaller than the volume of the pH gradient, V_g, so that we set $V_L/V_g = 0.01$. The pH difference across the whole gradient volume is set to $\delta(\mathrm{pH}) = 5$ pH units and the $[-d\mu/d(\mathrm{pH})]/\bar{\mu}$ term is set in the range from 1 to 10 pH^{-1} for good ampholytes (e.g., proteins and small net mobility). Then, Eq. 31 gives ϵ in the range from -10 to -100. Such a value of ϵ indicates that the zone is far from the steady state in the funnel-shaped

segment and thus Eqs. 30 and 32 derived above are not applicable. This statement also means that the influence of a secondary (=focusing) gradient is small in comparison with the influence of non-uniform geometry. In other words, it means that the first term in the denominator on the RHS of Eq. 12 (i.e., the dv/dy term) can be neglected in comparison with the second term. This approximation leads to Eq. 15. The dispersion of the zone can then be treated similarly as in Section 3.2. However, Eq. 21 should be used for the estimation of σ_0^2. It may be concluded that in electrofocusing methods with mobilization, the use of capillaries with a marked local increase in cross-section will have similar features to their use in zone electrophoresis.

The case of $q > 1$ and $Z > 0$

This condition describes the relaxation of a focused Gaussian zone during its transport through a tapered capillary. Since we want to obtain a focused zone with a small departure from the steady state, the capillary taper should be shallow. For a constant length-based variance of the zone, $\sigma^2 = \sigma_0^2 = \sigma_\epsilon^2$, such a condition can be quantified by Eqs. 27 and 28 for $0 < \epsilon \ll 1$ [1]. Of practical importance is the case with $\sigma_0^2 > \sigma_\epsilon^2$ which is closer to the loading of a real sample on the inlet of the tapered capillary. As indicated previously [22,23], soon after switching the current on, the components of the natural gradient are expected to order themselves according to their p*I* and an almost smooth natural pH gradient is formed. However, the actual width of the zone is far from that corresponding to the local steady state. In order to present the changes in zone variance graphically, let us take the numerical values as follows: $q = 10$ and the ratio of the total volume of the capillary, V_L, to the volume of the pH gradient, V_g, $V_L/V_g = 5$ [1]. Since V_g is regarded as a constant, the length of the pH gradient close to the injection point, V_{g0}, can be described with the help of relationships which are similar to Eqs. 5–7. L_{g0}, defined as $L_{g0} = y_{g0} - y_0$, may be written as (see Fig. 1b)

$$L_{g0} = \frac{V_L}{A_d} \cdot \frac{q^{V_g/V_L} - 1}{q \ln q} \tag{33}$$

When we take the typical values of $V_L = 1$ μl and $A_d = 0.01$ mm^2, we obtain from Eq. 33 $L_{g0} = 2.5$ mm for $q = 10$ and $V_L/V_g = 5$. Now, when we take $\sigma_\epsilon = 0.2$ mm, it appears that $(L_{g0}/\sigma_\epsilon)^2$ is about 150 (or $\sigma_{g0}^2/\sigma_\epsilon^2 = 13$), which allows us to use Eqs. 28–32 to estimate the dynamics of focusing during the entire transport of a sample from the capillary inlet toward the detection point (see discussion in Section 3.3). Thus, when the analyte is sampled together with background polyampholytes and the centre of its zone has a constant pH, its focusing can be estimated as described by Eq. 32.

In Fig. 6, the ratio $\sigma^2/\sigma_\epsilon^2$, the ratio of the concentration at the peak maximum, c_m, to the sampled concentration, c_0, expressed as c_m/c_0, and the actual peak position, $y - y_0$, are displayed as function of V/V_L for $\epsilon = 0.2$ and $(\sigma_0^2/\sigma_\epsilon^2 - 1) = 12$. Despite the numerous simplifications made in the calculations above, it can be concluded from the $\sigma^2/\sigma_\epsilon^2$ vs. V/V_L dependence calculated from Eq. 32 that the length-based variance of the analyte zone is expected to decrease rapidly so that it should approach σ_ϵ^2 after the displacement of a small fraction of V_L.

The distance of zone centre from the capillary inlet, $y - y_0$, as a function of the displaced volume is calculated with the help of Eqs. 5–7 similarly to Eq. 33 as

$$y - y_0 = \frac{V_L}{A_d} \cdot \frac{q^{V/V_L} - 1}{q \ln q} \tag{34}$$

It is apparent from the graph in Fig. 6 that the position of the zone changes slowly close to the capillary inlet and the zone moves faster when approaching the detection point at the narrower end of the capillary.

The ratio of the analyte concentration at the peak maximum to the uniform concentration in the volume of sampled solution was estimated from the mass balance as

$$\frac{c_m}{c_0} = \frac{V_g}{A\sigma\sqrt{2\pi}} \tag{35}$$

The dependence of the standard deviation of the zone on displaced volume was calculated from Eq. 32 and the dependence of the local cross-

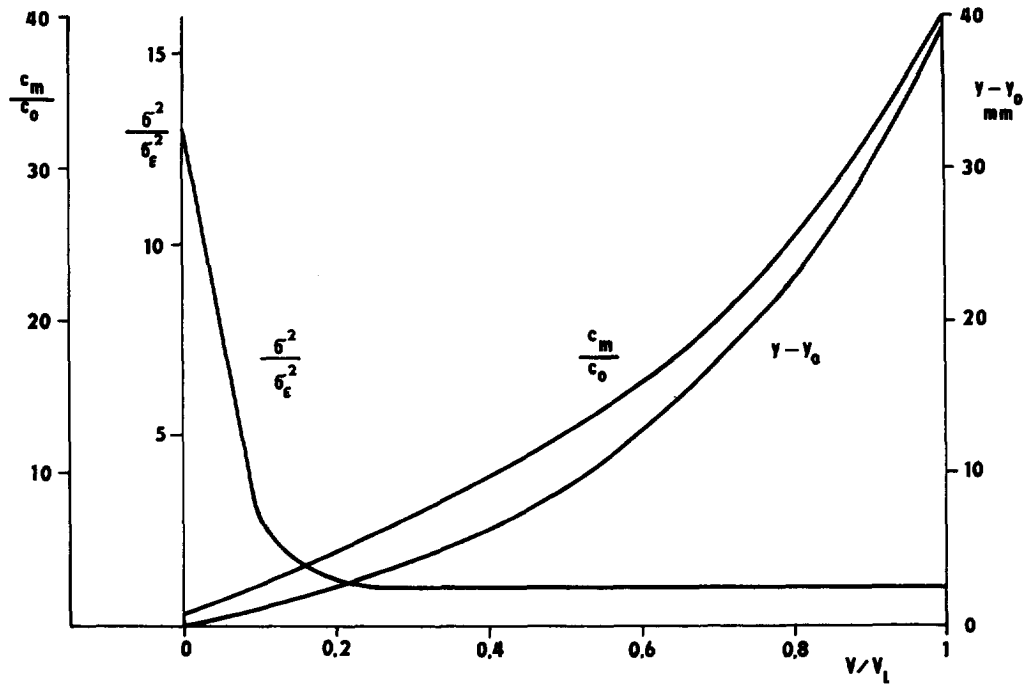

Fig. 6. Relaxation of a focused peak in a tapered capillary. $y-y_0$ = Distance of the peak from the capillary inlet calculated from Eq. 34; c_m/c_0 = ratio of concentration at the peak maximum to sampled concentration calculated from Eq. 35; $\sigma^2/\sigma_\epsilon^2$ = ratio calculated from Eq. 32. Symbols as in Figs. 1 and 3.

section on displaced volume from Eq. 8. It is apparent from the dependence of c_m/c_0 on V/V_L, shown in Fig. 6, that the concentration in the peak maximum increases continuously as the peak moves into positions with a smaller A. This phenomenon has been pointed out previously [1], and it follows from the conclusion that σ_ϵ is constant in a capillary with the geometry defined by Eqs. 5–7 (see Eq. 27).

Since the chosen ϵ equals 0.2, the zone should be close to the steady state at the outlet of the tapered capillary (see Eq. 28). A zone which is even closer to the steady state can be obtained when the outlet cross-section of a tapered capillary is coupled with the same cross-section of a capillary with uniform geometry (see Fig. 4). The changes in the zone variance in this coupled capillary were discussed in Section 3.3. The coupled uniform capillary can not only be convenient for improvement of the zone shape but also it can be important for detection [5] since uniform shapes can be made more easily, e.g., fused-silica capillaries for optical detection.

4. Conclusions

The equations derived support the unity of electrophoretic methods which lead to Gaussian zones, namely CZE and IEF. Despite the limitation to a special shape of the capillary and a number of simplifications, the present analytical solution appears to go beyond the classical treatments of CZE and IEF in the direction towards a description of transient processes.

The applications of the derived equations to practically interesting cases show the basic features of electrophoresis in capillaries of non-uniform cross-section and the possible directions for the improvement of electrophoretic methods. More complicated shapes can be treated as being

composed of funnel-shaped, tapered and uniform segments of the capillary.

The theoretical treatment of square-wave zones in a tapered capillary was published elsewhere [4].

Acknowledgement

This work was partially supported by a grant of the Academy of Sciences of the Czech Republic, No. A 4031504.

Symbols

A	Local cross-section of the capillary, variable (m^2)
A_0	Capillary cross-section at the inlet point (m^2)
A_d	Capillary cross-section at the detection point (m^2)
c_m	Concentration of focused ampholyte in zone maximum, variable (mol m^{-3})
c_0	Concentration of focused ampholyte in sampled volume V_g (mol m^{-3})
D	Diffusion coefficient, constant (m^2 s^{-1})
D^*	Effective dispersion coefficient, variable (m^2 s^{-1})
E	Field strength, variable (V m^{-1})
I	Electrical current, constant (A)
L	Length of capillary from y_0 to y_d (m)
L_{g0}	Initial length of natural pH gradient from y_0 to y_g (m)
q	Ratio of inlet to detection capillary cross-section (Eq. 7), dimensionless
r_0	Capillary radius at the inlet point (m)
r_d	Capillary radius at the detection point (m)
t	Time, variable (s)
t_a	Time of zone migration in uniform capillary prior entering the non-uniform capillary (s)
t_L	Time of migration of zone from y_0 to y_d (s)
v	Local migration velocity, variable (m s^{-1})
$\bar{v}$	Linear velocity of the zone mean, variable (m s^{-1})
$\bar{v}_0$	Linear velocity of the zone mean at capillary inlet (m s^{-1})
V	Volume displacement, variable (m^3)
V_L	Capillary volume from the inlet point to the detection point (m^3)
V_a	Volume of uniform capillary connected to inlet of non-uniform capillary (m^3)
V_g	Volume of natural pH gradient, constant (m^3)
y	Length coordinate along the capillary axis variable (m)
y_0	Coordinate of the capillary inlet (m)
y_d	Coordinate of the detection point (m)
y_{g0}	Coordinate of front of natural pH gradient at the start of focusing run (m)
Z	Constant defined by Eq. 12, dimensionless
δ(pH)	pH difference over volume of natural pH gradient, V_g, constant (pH)
ϵ	Parameter defined by Eq. 28, dimensionless
μ	Local effective mobility, variable (m^2 V^{-1} s^{-1})
$\bar{\mu}$	Effective mobility of the zone mean, constant (m^2 V^{-1} s^{-1})
σ	Actual length-based standard deviation of Gaussian zone (m)
σ_V	Actual volume-based standard deviation of Gaussian zone (m^3)
σ_s	Local steady-state length-based standard deviation of Gaussian zone (m)
σ^2	Actual length-based variance of Gaussian zone (m^2)
σ^2_{Lg}	Length-based variance of natural pH gradient at the beginning of the focusing run (m^2)
σ^2_s	Local steady-state length-based variance of Gaussian zone (m^2)
σ^2_t	Actual time-based variance of Gaussian zone (s^2)
σ^2_{t0}	Time-based variance of Gaussian zone at capillary inlet (s^2)
σ^2_V	Actual volume-based variance of Gaussian zone (m^6)
σ^2_0	Length-based variance of zone at capillary inlet (m^2)

σ_ϵ^2 Length-based variance of zone defined by Eq. 27 (m^2)

Φ Volume velocity of migration, volume displacement of the zone per time unit, constant ($m^3\ s^{-1}$)

References

[1] K. Šlais, J. Chromatogr. A, 684 (1994) 149.
[2] K. Šlais, in Proceedings of the 16th International Symposium on Capillary Chromatography, Riva del Garda, September 1994, p. 1815.
[3] K. Šlais, J. Microcol. Sep., 7 (1995) 127.
[4] K. Šlais, Electrophoresis, 16 (1995) 2060.
[5] M. Šťastná, V. Kahle and K. Šlais, J. Chromatogr. A, 730 (1996) 261.
[6] J. Pawliszyn and J. Wu, J. Microcol. Sep., 5 (1993) 397.
[7] D.N. Heiger, P. Kaltenbach and H.-J.P. Sievert, Electrophoresis, 15 (1994) 1234.
[8] Y. Xue and E.S. Yeung, Anal. Chem., 66 (1994) 3575.
[9] W. Beck, C. Büttner, S. Adam and H. Engelhardt, presented at the 6th International Symposium on HPCE, San Diego, CA, February 1, 1994.
[10] C.D. Bevan, and I.M. Mutton, presented at the 20th International Symposium on Chromatography, Bournemouth, June 1994; J. Chromatogr. A, 679 (1995) 541.
[11] G.H. Weiss, N. Catsimpoolas and D. Rodbard, Arch. Biochem. Biophys., 163 (1974) 106.
[12] N. Catsimpoolas, Sep. Sci., 10 (1975) 55.
[13] N. Catsimpoolas, Anal. Biochem., 54 (1973) 79.
[14] N. Catsimpoolas, W.W. Yotis, A.L. Grffith and D. Rodbard, Arch. Biochem. Biophys., 163 (1974) 113.
[15] V. Dolník, M. Deml and P. Boček, J. Chromatogr., 320 (1985) 89.
[16] J.C. Giddings, Unified Separation Science, Wiley-Interscience, New York, 1991.
[17] H. Svensson, Acta Chem. Scand., 15 (1961) 325.
[18] C. Giddings and K. Dahlgren, Sep. Sci., 6 (1970) 345.
[19] K. Šlais, J. Microcol. Sep., 5 (1993) 469.
[20] M. Dishon, G.H. Weiss and D.A. Yphantis, Biopolymers, 10 (1971) 2095.
[21] M. Dishon and G.H. Weiss, Anal. Biochem., 81 (1977) 1.
[22] W. Thormann and R.A. Mosher, in A. Chrambach, M.J. Dunn and B.J. Radola (Editors), Advances in Electrophoresis, Vol. 2, VCH, Weinheim, 1988, p. 45.
[23] R.A. Mosher, D.A. Saville and W. Thormann, The Dynamics of Electrophoresis, VCH, Weinheim, 1992.